ADVANCING EARTH AND SPACE SCIENCES

Geophysical Research Letters

RESEARCH LETTER
10.1029/2025GL120943

Pacific Decadal Oscillation Modulates an Interdecadal Trans-Pacific Dry-Wet Seesaw in East Asian and North American Semi-Arid Regions

Shanshan Wang[1,2], Xinya Shu[1], Jianping Huang[1,2], Jinfei Sun[1], and Fuxing Shi[1]

[1]Key Laboratory for Semi-Arid Climate Change of the Ministry of Education, College of Atmospheric Sciences, Lanzhou University, Lanzhou, China, [2]Collaborative Innovation Center for Western Ecological Safety, Lanzhou University, Lanzhou, China

Key Points:

- PDO forces an interdecadal dry-wet seesaw between East Asian and North American semi-arid regions
- PDO phase shifts trigger a teleconnection pattern that modulates East Asian monsoon and westerlies, thereby modifying moisture transport
- This causal linkage provides a mechanistic basis for improving decadal-scale hydroclimatic risk prediction in vulnerable semi-arid lands

Supporting Information:

Supporting Information may be found in the online version of this article.

Correspondence to:

J. Huang,
hjp@lzu.edu.cn

Citation:

Wang, S., Shu, X., Huang, J., Sun, J., & Shi, F. (2026). Pacific decadal oscillation modulates an interdecadal trans-Pacific dry-wet seesaw in East Asian and North American semi-arid regions. *Geophysical Research Letters*, *53*, e2025GL120943. https://doi.org/10.1029/2025GL120943

Received 2 DEC 2025
Accepted 3 APR 2026

Abstract Semi-arid regions are expanding globally through divergent pathways: in East Asia (EA) via drying of semi-humid lands, while in North America (NA) through wetting of arid areas. This interdecadal dry-wet reversal across the Pacific has remained mechanistically unclear. Here we demonstrate that the Pacific Decadal Oscillation (PDO) drives this climatic seesaw. Analysis of 1948–2022 data reveals the PDO explains approximately 21% of dry-wet variance in EA and 63% in NA. We identify a trans-Pacific teleconnection where PDO phase transitions generate key atmospheric anomalies—a summer Eurasian anticyclone and winter-deepened Aleutian Low—that subsequently modify East Asian monsoons and westerly flows. This atmospheric reorganization alters moisture transport patterns, ultimately producing opposing hydroclimatic trends across the continents. Our work establishes a causal relationship between PDO phase shifts and interdecadal dry-wet reversals, providing crucial mechanistic understanding for predicting long-term hydroclimatic risks in vulnerable semi-arid regions under natural climate variability.

Plain Language Summary Semi-arid regions are important ecological zones that have been expanding around the world. Interestingly, while semi-arid regions in East Asia have become drier, those in North America have become wetter over multi-decadal timescales, creating a "climate seesaw" across the Pacific. The reason for this opposite behavior has been poorly understood. Our study finds that the Pacific Decadal Oscillation (PDO), a long-term pattern of Pacific Ocean temperature variability, is the primary driver of this phenomenon. We show that when the PDO shifts from one phase to another, it triggers changes in key weather systems, like strengthening high pressure over Eurasia and deepening low pressure over the Aleutian Islands. These changes, in turn, weaken the East Asian monsoon and alter the westerly winds, ultimately redirecting moisture transport. This mechanism causes drought in East Asia and wet conditions in North America, or vice versa. Our research provides a scientific explanation for this interdecadal climate seesaw, which is crucial for improving long-term hydroclimatic risks forecasting and water resource management in these vulnerable regions.

1. Introduction

Semi-arid regions cover about 15% of the Earth's land area, receiving relatively low amounts of precipitation with sparse vegetation. Nevertheless, these regions are important agricultural and pastoral areas, and feed more than 14% of the global population (Safriel and Adeel, 2005). The ecosystems in such regions are vulnerable and sensitive to human interventions, climate changes (e.g., Chen et al., 2025; Hu et al., 2025; Huang, Ji, et al., 2015; Rotenberg and Yakir, 2010; Zeng et al., 1999) and climate variability, especially to the increasing risk of extreme events such as heat waves, torrential precipitation and drought in a warming climate (IPCC, 2013, 2023; Zhang et al., 2023). Based on observational and simulation results, Chen et al. (2022) indicated that drylands have expanded over the past half-century and that this trend will persist into the 21st century. Specifically, more than half of the total dryland expansion is contributed by the semi-arid land expanding (Feng & Fu, 2013; Huang, Ji, et al., 2015, Huang, Li, et al., 2017, Huang, Thorne, et al., 2017, Huang, Yu et al., 2015). However, there are noticeable differences in dry/wet trends over different semi-arid regions. For example, North China experiences a drying trend since 1950s (e.g., Cui et al., 2021; Jin et al., 2025; Qian and Zhou, 2014; Zhang and Zhou, 2015;), while the western North America presents a wetting trend during the same period (e.g., Akinsanola et al., 2024; Dai, 2013; Fan et al., 2025; Jamali et al., 2023). Further, Huang, Ji, et al. (2015), Huang, Li et al. (2017), Huang, Thorne, et al. (2017) found that the newly formed semi-arid regions across the North America (NA) is developed from arid regions due to the wetting climate, while semi-arid expansion in East Asia (EA) is mainly contributed by the drying of sub-humid/humid regions during the latter half of the 20th Century. Entering into 21st Century, the precipitation in semi-arid regions of EA has started to increase, with the eastward expansion of wetting trend in northwest China (Wang et al., 2022; Zhang et al., 2022). In contrast, semi-arid regions in NA have been frequently hit droughts (Mann and Gleick, 2015). That is, the dry/wet trends are reversed over the semi-arid regions in EA and NA at interdecadal timescales.

However, the reason for this interdecadal reversal in dry/wet trends over EA and NA semi-arid regions has not been explicitly discussed. Previous studies have noted that the Pacific decadal oscillation (PDO), also referred to as the Interdecadal Pacific Oscillation (IPO), not only plays a crucial role on the dry/wet changes over southwestern America (e.g., Dai, 2013; Dong & Dai, 2015; Gershunov & Barnett, 1998; McCabe et al., 2004; Seager et al., 2023; Yu and Zwiers, 2007), but also links closely to the climate change over East Asia (e.g., Qian and Zhou, 2014; Wang et al., 2024; Yu et al., 2015). For instance, Seager et al. (2023) observed that the warm phase of the PDO contributed to the wetting of the southwestern United States during the late 20th century by modulating cool season precipitation through tropical Pacific SST forcing. Conversely, during the cold PDO phase, a strong high pressure center and anti-cyclonic anomaly circulation is very visible over the North Pacific in the lower troposphere, which lead to dry and cold northwesterly and northerly winds and below-normal precipitation over much of the West US (Dai, 2013). Li et al. (2010) suggested that the interdecadal PDO-like sea surface temperature (SST) anomalies pattern is a major cause for the weakening of the East Asia summer monsoon (EASM) during recent decades, thereby influencing China's climate. Furthermore, recent studies indicate that the PDO can influence global and regional precipitation variability by modulating the interactions between ENSO and the Asian summer monsoon (Fuentes-Franco et al., 2016; Wang et al., 2024). Therefore, PDO might also be relevant to the dry/wet trends over the two semiarid regions as a regulator or a bridge over the Asia-Pacific-America region.

In fact, the teleconnection involved with PDO between EA and NA climate variability in both winter (Cohen & Entekhabi, 1999; Ge et al., 2024; Lee et al., 2025; Li et al., 2019; Yang et al., 2002) and summer (Guo et al., 2024; Lau and Weng, 2002; Lau et al., 2004; Si et al., 2021; Yan et al., 2022) have been discussed by some studies, but there is no or little attention paid on the semi-arid regions, which are very sensitive to climate change. This work will explore the possible linkage between the reversed dry/wet trends and PDO via the Asia-Pacific-North America teleconnection, address the possible mechanism under a warming climate, and provide an alternative approach for facilitating decadal predictions over semi-arid regions.

2. Data and Method

The monthly PDO index, obtained from the National Oceanic and Atmospheric Administration (NOAA, https://www.ncei.noaa.gov/access/monitoring/pdo/), is derived from the ERSST Version 5 data set (ERSSTv5; Huang, Li, et al., 2017, Huang, Thorne, et al., 2017), which is also the monthly SST data set used in this study. It is defined as the standardized leading principal component of the EOF analysis of monthly sea surface temperature anomalies in the North Pacific (north of 20°N) (Mantua et al., 1997; Zhang et al., 1997). Before the EOF analysis, the monthly mean global average SST anomalies have been removed to separate this pattern of variability from any global warming signal.

The semi-arid regions in this study are defined as the climatological aridity index (AI) for 1961–1990 is less than 0.5 and greater than 0.2 (e.g., Feng & Fu, 2013; Huang, Ji, et al., 2015, Huang, Yu et al., 2015). Here the AI is defined as the ratio of annual precipitation and annual potential evapotranspiration, and represents the degree of climatic dryness, which is provided by Feng and Fu (2013) for the period of 1948–2008. Meanwhile, the monthly variation for AI can measure the dry/wet changes in one region as well.

The precipitation, potential evapotranspiration, and surface air temperature data were sourced from the Climatic Research Unit gridded Time Series (CRU TS), version 4.09 (Harris et al., 2020). In addition, the circulation data, including geopotential height and horizontal winds, as well as the vertical integral water vapor flux, are derived from the ERA5 reanalysis (Hersbach et al., 2020). This study focuses on the full cold-to-warm-to-cold phase transition cycle of the PDO from 1948 to 2022, marked by climatic regime shifts in 1976/77 and 1998/99. We examine two key transition periods of PDO phase: P1 (1948–1998), encompassing the shift from a negative to a

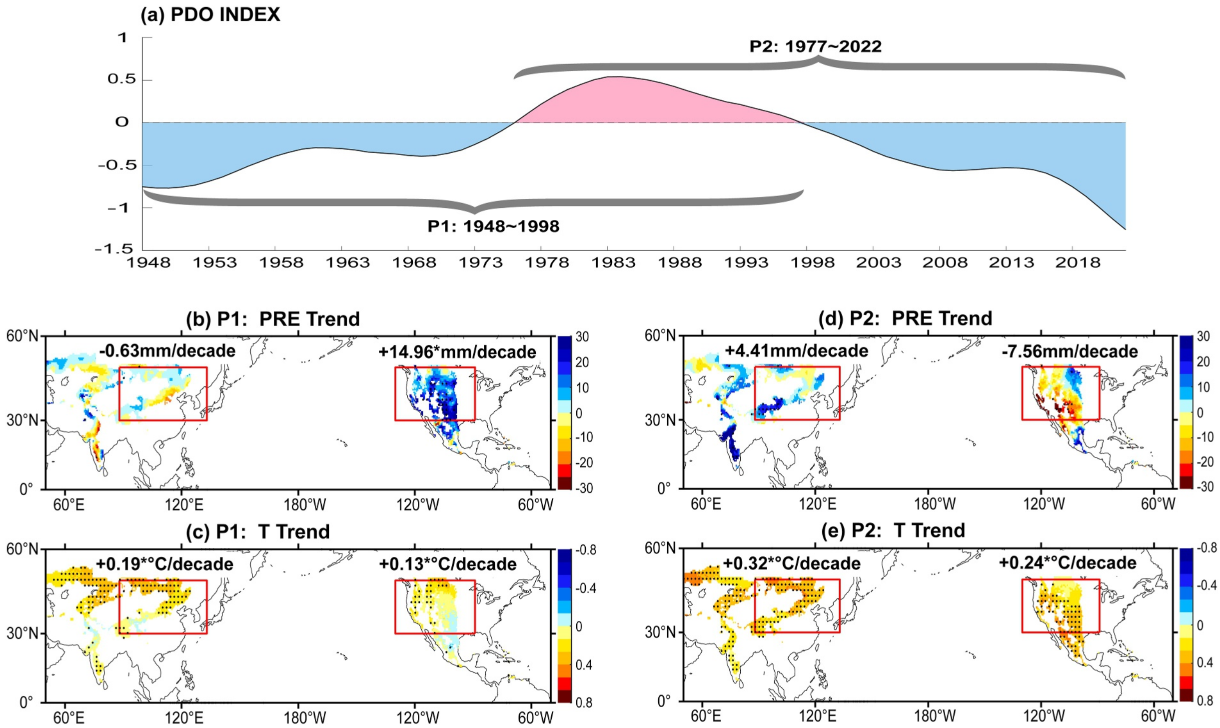

Figure 1. (a) Time series of the 21-year smoothed PDO index. Analysis periods P1 (1948–1998) and P2 (1977–2022) are indicated. The distributions of the linear trends in annual precipitation and annual mean temperature in semiarid regions over East Asia and North America from 1948 to 2022, covering one full cycle of the PDO (1948–1976 and 1999–2022: cold phase; 1977–1998: warm phase). (b and d) Precipitation trend (mm/decade); (c and e) temperature trend (°C/decade). An asterisk indicates the trend is statistically significant at the 95% confidence level (two-tailed *t*-test).

positive phase, and P2 (1977–2022), covering the transition from a positive to negative phase, as shown in Figure 1a.

Maximum covariance analysis (MCA; Frankignoul et al., 2011; Barreto et al., 2017) is applied to examine the relationship between precipitation over semi-arid East Asia (EA) and North America (NA) and the global SST field (1948–2022). As a common climate statistical method, MCA decomposes the temporal cross-covariance matrix of two physical fields via singular value decomposition (SVD), isolating the most coherent spatial pattern pairs and their time series to clarify the linkages between semi-arid precipitation and global SST anomalies.

To investigate the forcing impacts of PDO phase transitions on atmospheric teleconnection patterns, a series of sensitivity experiments were conducted using the Community Atmosphere Model version 6 (CAM6.0). The model was configured with a horizontal resolution of 0.9° latitude × 1.25° longitude and 32 hybrid $\sigma{-}p$ vertical levels. Using the Climo2000 component of CAM6, we performed 50 ensemble members for each of the two experimental setups (Table 1). To ensure the statistical robustness of the results and to mitigate transient effects arising from initial conditions and model spin-up, only the final 35 years of simulation output from each ensemble member were used for analysis.

Table 1
Experimental Design for CAM6.0 Sensitivity Simulations

Experiments	Experimental design	Duration	Results
Control experiment (EXP_CTL)	Forced operation based on observed monthly SST climate averages (1981–2010 averages)	50-runs	PDO-CTL
PDO experiment (EXP_PDO)	Same as EXP_CTL, but the forcing uses the composite SST difference between the observed warm (1977–1998) and cold (1948–1976) PDO phases, superimposed on the climatological SST.		

The control experiment (EXP_CTL) is forced by 1981–2010 monthly climatological SSTs with default sea ice, while the sensitivity experiment (EXP_PDO) was designed to isolate PDO-related SST forcing effects, superimposing monthly North Pacific (0–70°N, 120°E−90°W) SST anomalies (warm minus cold PDO phases) onto EXP_CTL's SSTs (preserving seasonal cycles), with all other settings identical to EXP_CTL.

3. Results

3.1. Interdecadal Seesaw Pattern in Dry–Wet Trends Over Semi-Arid EA and NA

Semi-arid regions in EA and NA are both located in the mid-latitudes of the North Hemisphere and have experienced enhanced warming since 1948 (Huang, Ji, et al., 2015; Huang, Yu et al., 2015, Huang et al., 2012). The climate over EA is mainly influenced by the monsoon circulation, characterized by seasonal reversals in wind and precipitation patterns—even within the semi-arid regions, particularly along their southern and eastern edges (Figure S1 in Supporting Information S1). Summer rainfall accounts for more than half of the annual precipitation in the EA semi-arid region (Figure S2 in Supporting Information S1). In contrast, precipitation in NA is largely dominated by moisture transported via westerly winds (Figure S1 in Supporting Information S1)—with less precipitation in summer and most concentrated in spring, autumn, and winter, particularly in winter (Figure S2 in Supporting Information S1).

Figure 1 shows the linear trends in the precipitation and temperature across the semi-arid regions over EA and NA during the two sub-periods P1 and P2. Obviously, there is a reversed relationship in the dry/wet trends over the two semi-arid regions. During P1, which coincides with the cold-to-warm PDO transition, the semi-arid region of EA experienced a drying trend. This was characterized by a decrease in precipitation (−0.63 mm/decade) accompanied by significant warming (+0.19°C/decade), thereby exacerbating the aridity through enhanced evapotranspiration. Over the same period, the NA semi-arid region also warmed considerably; however, precipitation increased markedly (+14.96 mm/decade), resulting in a moistening trend.

In P2, corresponding to the warm-to-cold PDO transition, the dry–wet relationship reversed between the two regions: EA shifted toward wetter conditions (+4.41 mm/decade), whereas NA exhibited a drying trend (−7.56 mm/decade). Temperature continued to rise significantly in both regions throughout P2.

Overall, an interdecadal seesaw pattern in dry–wet variations is clearly identified between the semi-arid regions of EA and NA. This dipole-like trend was previously noted by Huang, Ji, et al. (2015) for 1948–2008. Our extended analysis indicates that the drying in EA and wetting in NA during that period were largely associated with the cold-to-warm phase shift of the PDO around 1976/77. Toward the end of the 20th century, the PDO shifted back to a cold phase, triggering increased precipitation and a eastward-expanding tendency toward warmer-wetter conditions in EA, alongside more frequent droughts in NA.

3.2. Dominant Role of PDO in Driving the Interdecadal Dry–Wet Seesaw

As mentioned in the introduction and Section 3.1, the PDO may play a crucial role on the interdecadal seesaw pattern of dry/wet variability observed between the two semi-arid regions. To diagnose this connection, the MCA is carried out to isolate the dominant mode of the co-variability between SST anomalies and the dry/wet variations over the semi-arid regions of EA and NA from 1948 to 2022 (Figure 2). Results show that the first robust mode (MCA1) for EA semi-arid region represents global warming, accounting for 54% of the total variance (not shown), and the second mode of MCA shows a PDO-like SST pattern (Figure 2a), which explains 21% of the total variance. Moreover, the time series corresponding to this SST pattern is significantly correlated with the standardized PDO time series, with an original correlation coefficient of 0.69 ($p < 0.01$). Its corresponding PRE field shows one-sign drying over most of the EA semi-arid region (Figure 2b). In contrast, the leading mode for NA is dominated by a PDO-like SST pattern, explaining about 63% of the covariance, and is associated with a one-sign wetting pattern across the NA semi-arid region (Figures 2c and 2d). These results indicate that long-term dry/wet variation over the semi-arid regions of EA is more sensitive to global warming and the PDO phase transition is the secondary diver at interdecadal timescale. Conversely, the PDO serves as the dominant factor governing wet-to-dry transition in semi-arid NA during the same period. These findings provide a crucial insight for future decadal climate prediction in the two semi-arid regions in the future.

To further elucidate the linkage between the PDO and the interdecadal dry/wet seesaw, we examined associated circulation anomalies with PDO across the Asia-Pacific-America sector. Considering that precipitation in East

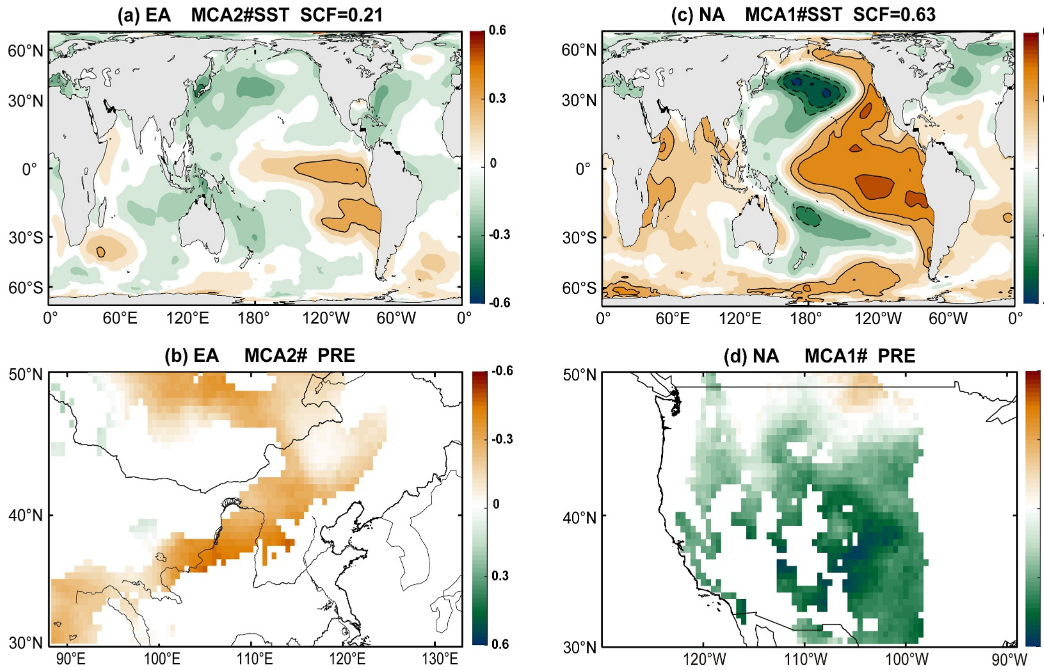

Figure 2. Spatial patterns of the MCA between global SST and precipitation (PRE) in semi-arid regions during 1948–2022, based on annual mean SST and annual total precipitation. (a) The global SST anomaly pattern of the second MCA mode and (b) the corresponding precipitation anomalies over semi-arid East Asia; (c) the global SST anomaly pattern of the first MCA mode and (d) the corresponding precipitation anomalies over semi-arid North America. In (a) and (c), solid (dashed) contours denote positive (negative) values, with intervals from 0.3 to 1.0 and 0.3 to −1.0, respectively. The fraction of explained covariance for each mode is indicated in the top-right corner of (a) and (c).

Asia is dominated by summer, while precipitation in the North American arid regions is westerly driven—with less precipitation in summer and most concentrated in spring, autumn, and winter, particularly in winter—we focus on the circulation changes associated with PDO phase shifts in summertime and wintertime. Figures 3a

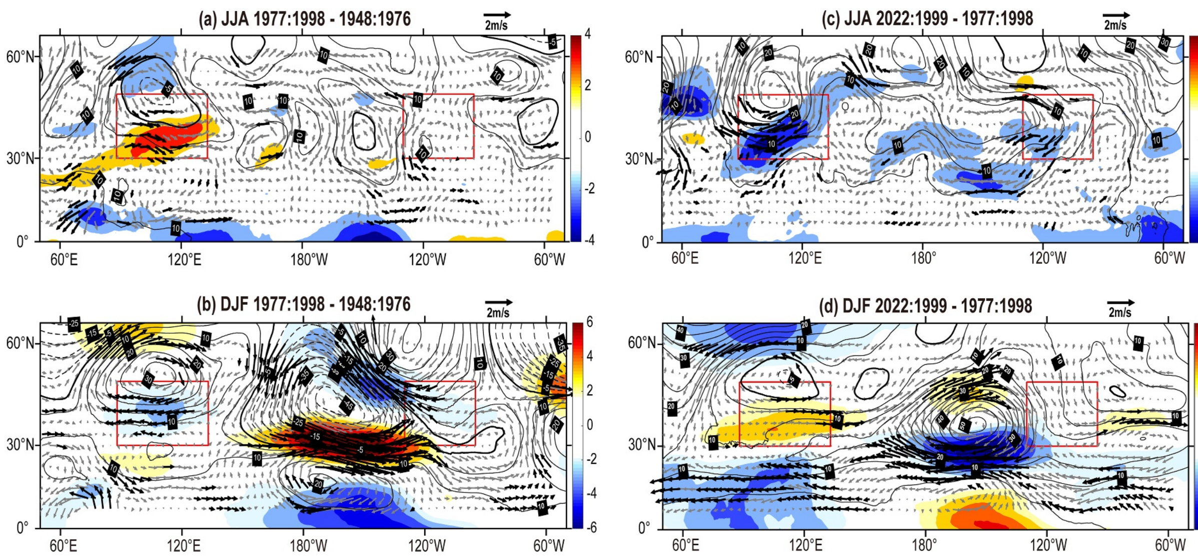

Figure 3. Composite differences in atmospheric circulation between cold and warm phases of the PDO for boreal JJA and DJF. (a), (b) Cold-phase minus warm-phase composites for P1 (cold phase: 1948–1976; warm phase: 1977–1998) derived from the ERA5 reanalysis. Contours denote geopotential height anomalies (units: gpm; interval: 5 gpm) and vectors represent the 500-hPa wind (m/s), and shading indicates 200-hPa zonal wind anomalies (units: m/s). (c), (d) As in (a), (b), but for P2 (cold phase: 1999–2022; warm phase: 1977–1998). Thick black contours enclose regions where the composite difference is statistically significant at the 90% confidence level based on a two-tailed Student's *t*-test.

and 3b show differences in 500 hPa geopotential height and wind and 200 hPa zonal wind, between the warm phase (1977–1998) and the cold phase (1948–1976) of PDO during boreal summertime (June-July-August, JJA) and wintertime (December-January-February, DJF). For JJA, a strong high-pressure anomaly dominated the Asian continent, centered near in the Balkhash Lake. To the east of this center, anomalous northerly and northwesterly substantially weaken the climatological moist southeasterly from the Pacific, that is, a weakened EASM. This circulation pattern prevents moisture transport into the EA semi-arid region, reducing precipitation (Figure S4 in Supporting Information S1). Another predominant feature is the enhanced and southward-shifted East Asia jet stream near 30°–40°N (Lau et al., 2004). The intensified jet is accompanied by enhanced subsidence to the north, further suppressing rainfall in the EA semi-arid region. Additionally, an abnormally cyclone concomitant with a relative weaker low pressure in eastern Pacific along the western coast of NA allows more moisture transporting into the semi-arid region in NA.

In DJF, a similar high-pressure anomaly like JJA prevails over Asia, strengthening the East Asia winter monsoon (EAWM) and advecting dry and cold air that reduces precipitation over semi-arid EA. In contrast, an abnormally deep low pressure dominates the North Pacific, particularly around the Aleutian island (Figure 3b). This deepened Aleutian Low intensifies westerlies along its southern flank and leads to a more southerly, zonal, and strengthened upper-level jet (Yang et al., 2002, Dai et al., 2013). This circulation anomaly enhances the Pacific/North American teleconnection pattern (PNA), channeling more moisture into the NA semi-arid regions (Figure 3b; Figure S4 in Supporting Information S1). Similar modulations by the Aleutian Low and its southern westerlies are also evident in spring and autumn, contributing to the precipitation changes and reinforcing the opposite precipitation trends between East Asia and North America (Figure S3 in Supporting Information S1). Additional moisture from the Atlantic, associated with a slight cyclonic anomaly over the Gulf of Mexico, converges over the western U.S., resulting in increased precipitation.

Figures 3c and 3d present the composite circulation differences for the P2 period, during which the PDO transitioned from its warm to cold phase. In JJA, EA experiences a weakened jet stream and enhanced easterly winds, reinforcing the EASM and intensifying moisture transport from the Pacific, which increases precipitation over the East Asian semi-arid region (Figures 3c and 3d). Meanwhile, a cyclonic anomaly and a weak anticyclonic center over the western coast of NA reduce moisture delivery, decreasing rainfall in the NA semi-arid region. During DJF, the intensified Hawaiian High enhances the southward intrusion of dry, cold air into North America, accompanied by strengthened subsidence, further suppressing moisture and reducing precipitation.

3.3. Model Verification of PDO's Impact on Interdecacal Dry–Wet Seesaw

To systematically evaluate the forcing effect of PDO phase transitions on the reversed dry-wet variability over the semi-arid regions of EA and NA during 1948–2022, a set of sensitivity experiments was conducted using the CAM6.0. The experimental design involved superimposing the observed SST anomaly pattern—defined as the composite difference between the typical PDO warm (1977–1998) and cold (1948–1976) phases—onto the monthly climatological SST field to isolate the atmospheric response to PDO-related SST forcing. Detailed experimental configurations are summarized in Table 1.

The model successfully reproduced key large-scale circulation changes in summer and winter associated with the PDO cold-to-warm phase shift, as well as the corresponding precipitation responses over EA and NA. In JJA, the simulation captured an anomalous anticyclonic system over the mid-to high-latitudes of Eurasia, with a pronounced high-pressure center stabilized near the Aral Sea. The enhanced northerly and northwesterly flows on the eastern flank of this anticyclone facilitated the southward transport of dry, cold air, which suppressed the northward advance of the East Asian summer monsoon moisture, thereby leading to significantly reduced precipitation over the EA semi-arid region (Figure 4a). In DJF, the model simulated a deepened and eastward-extended Aleutian Low toward the North American west coast. The intensified westerlies on its southern flank, together with an anomalous cyclonic circulation over the southern part of North America, established a low-level channel that enhanced moisture transport from the tropical Pacific to the western continent. This resulted in a significant increase in precipitation, manifesting as widespread positive anomalies over the NA semi-arid region (Figure 4b). We also analyzed spring and autumn variations (Figure S3 in Supporting Information S1), and the results show that under the PDO cold-to-warm phase shift, the ascending low pressure deepens, and the westerly wind strengthens in its southern part (facilitating water vapor transport to western NA arid regions), which is consistent with the winter characteristics and yields similar conclusions. The spatial pattern of these

10.1029/2025GL120943

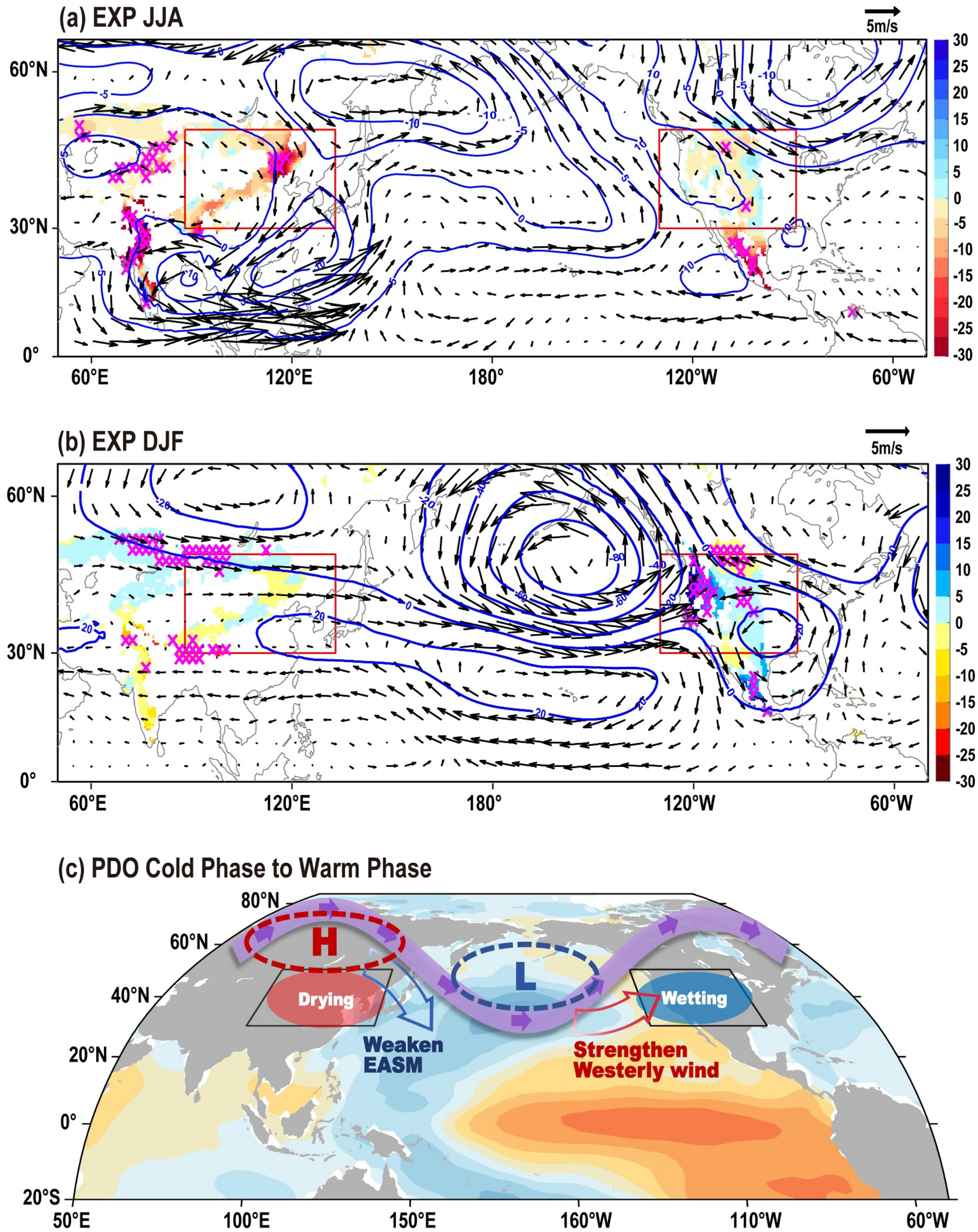

Figure 4. Composite differences in 500-hPa geopotential height (unit: m, contour) and wind (unit: m/s) and precipitation (unit: mm/month, shade) for JJA (a) and DJF (b) between the control and PDO experiments based on CAM6 (PDO-CTL). The pink dotted regions are statistically significant at the 90% confidence level. (c) Is a diagram of the mechanism by which PDO affects atmospheric circulation.

simulated responses is highly consistent with observations shown in Figure 1c, confirming the model's capability in capturing the circulation and precipitation responses under PDO forcing.

In summary, the numerical experiments successfully replicate the observed dry-wet seesaw and its associated circulation anomalies over the EA and NA semi-arid regions, demonstrating that the atmospheric response to PDO-related SST anomalies is a key process driving the dry-wet trends at interdecadal timescales in these regions (Figure 4c). Specifically, PDO-related SST anomalies can drive adjustments in atmospheric circulation patterns, alter key moisture transport pathways and modulate vertical motion, thereby exerting an important forcing effect on the interdecadal dry-wet variability over the two semi-arid regions. This study provides robust numerical evidence for understanding the role of PDO-related SST variability in shaping hydroclimatic conditions in semi-arid regions across the Northern Hemisphere.

4. Conclusion and Discussion

This paper investigates the mechanism on the PDO's contribution to the reversed relationship of the dry/wet trends at interdecadal timescale between the vulnerable semi-arid lands in the EA and NA from 1948 to 2022, which consists a full cycle of PDO cold-to-warm (1948–1998) and a full cycle of warm-to-cold PDO transition (1999–2022). Results show that about 21% (63%) of the dry/wet variance for the semi-arid region of EA (NA) is attributable to PDO based on the MCA analysis. As a regulator, the PDO shift is closely related to a teleconnection pattern spanning the entire Asian–Pacific–American region coupled with EA monsoon systems, westerly and subtropical jet, and PNA, etc. During the full cycle, the PDO shift from a cold to a warm phase is characterized with a cooling in the extratropical central North Pacific and a warming along the west coast of North America and Alaska (Mantua et al., 1997), which is always companied by the abnormally high pressure over Asia continent in both JJA and DJF and an anomalous low pressure center in the center North Pacific for DJF. In the lower and middle troposphere, these circulation patterns are conductive to weaken the EASM in summer and prohibit the moisture from Pacific to reach the semi-arid region of EA. They also strengthen the EAWM in winter, and consequently most of northern EA is dominated by the cold dry air, thereby resulting in the drying in EA. Meanwhile, they also accelerate the westerly and make the subtropical jet more southerly, zonally and stronger, which are conductive to more moisture into the semi-arid region of NA, thereby explaining the wetting trend in this region. In addition, the experimental results further demonstrate that the PDO influences dry-wet trends in the EA and NA semi-arid regions by inducing key seasonal atmospheric anomalies: a summer Eurasian anticyclone and a winter-deepened Aleutian Low.

Our study confirms that, at the end of the 20th century, when the PDO shifted again from the warm phase to the cold phase (Dong & Dai, 2015; Wang et al., 2014), the aridity in the EA semi-arid region and wetness in the NA region transitioned to wetness in the EA region and aridity in the NA semi-arid region. As mentioned above, the dry/wet variation in the semi-arid region in EA is more sensitive to the climate warming than NA, and the drying during the full PDO cycle is not only contributed by the PDO shift, but also due to the human-induced warming. As moving into the 21st century, the global warming appears a "new normal" (Trenberth et al., 2015) and the increasing rate for temperature seems slow down, as referred to as the "hiatus." So far, some researchers pointed out that the global warming is not stopping with the growing of CO2 emissions, the "hiatus" is just the result of the abnormally colder SST in the tropical Pacific, which links to the switch of the PDO from a warm to a cold phase (e.g., Guan et al., 2015; Kosaka and Xie, 2013; Trenberth, 2015). While our findings indicate a significant association between dry-wet regime shifts in the EA and NA semi-arid regions and the phase transitions of the PDO, it is important to note that the PDO itself is not a single physical process (Newman and Coauthors, 2016). Zhang et al. (2018) demonstrated that internal variability of the PDO played a critical role in the North Pacific climate system shift during the 1940s. Understanding the decadal-scale regulation of regional climate by such marine drivers represents a current frontier in climatology. This study thus provides an observational basis and mechanistic insight into the response of global semi-arid regions to natural low-frequency variability, with important implications for improving long-term drought risk prediction.

Conflict of Interest

The authors declare no conflicts of interest relevant to this study.

Availability Statement

All data supporting the findings of this study are publicly available from the following sources: The monthly Pacific Decadal Oscillation (PDO) index was obtained from the National Oceanic and Atmospheric Administration (NOAA) at https://www.ncei.noaa.gov/access/monitoring/pdo/. The aridity index (AI) data used to define semi-arid regions for the period 1948–2008 can be accessed by contacting the corresponding author of Feng and Fu (2013) via email. Precipitation, potential evapotranspiration, and surface air temperature data are from the

Climatic Research Unit (CRU TS v4.09), available at https://crudata.uea.ac.uk/cru/data/hrg/. Sea surface temperature data are from the NOAA Extended Reconstructed SST (ERSSTv5), available at https://www.ncei.noaa.gov/products/extended-reconstructed-sst. Atmospheric circulation data are from the ERA5 Reanalysis project, available at https://cds.climate.copernicus.eu/datasets.

Acknowledgments

This study is jointly supported by the National Science Foundation of China (42522503 and 42475023).

References

Akinsanola, A. A., Chen, Z., Kooperman, G. J., & Bobde, V. (2024). Robust future intensification of winter precipitation over the United States. *npj Climate and Atmospheric Science*, *7*(1), 212. https://doi.org/10.1038/s41612-024-00761-8

Barreto, N. J. C., Mesquita, M. d.S., Mendes, D., Spyrides, M. H. C., Pedra, G. U., & Lucio, P. S. (2017). Maximum covariance analysis to identify intraseasonal oscillations over tropical Brazil. *Climate Dynamics*, *49*(5–6), 1583–1596. https://doi.org/10.1007/s00382-016-3401-3

Chen, C., Wang, S., Wang, Z., & Li, X. (2025). Differential impacts of sub-daily precipitation on temperature extremes across China's climatic zones. *Geophysical Research Letters*, *52*(9), e2024GL114088. https://doi.org/10.1029/2024gl114088

Chen, Y., Li, Y., Li, Z., Liu, Y. C., Huang, W. J., Liu, X. G., & Feng, M. Q. (2022). Analysis of the impact of global climate change on dryland areas. *Advances in Earth Science*, *37*, 111–119. https://doi.org/10.11867/j.issn.1001-8166.2022.006

Cohen, J., & Entekhabi, D. (1999). Eurasian snow cover variability and Northern Hemisphere climate predictability. *Geophysical Research Letters*, *26*(3), 345–348. https://doi.org/10.1029/1998gl900321

Cui, Y., Zhang, B., Huang, H., Zeng, J., Wang, X., & Jiao, W. (2021). Spatiotemporal characteristics of drought in the North China Plain over the past 58 years. *Atmosphere*, *12*(7), 844. https://doi.org/10.3390/atmos12070844

Dai, A. (2013). The influence of the Inter-decadal Pacific Oscillation on U.S. precipitation during 1923-2010. *Climate Dynamics*, *41*(3–4), 633–646. https://doi.org/10.1007/s00382-012-1446-5

Dong, B., & Dai, A. (2015). The influence of the Inter-decadal Pacific Oscillation on temperature and precipitation over the globe. *Climate Dynamics*, *45*(9–10), 2667–2681. https://doi.org/10.1007/s00382-015-2500-x

Fan, X., Huang, J., Xie, Y., Wei, W., Ren, Y., Xu, Y., et al. (2025). External and internal controls on decadal precipitation variability over North America. *Climate Dynamics*, *63*(11), 429. https://doi.org/10.1007/s00382-025-07937-9

Feng, S., & Fu, Q. (2013). Expansion of global drylands under a warming climate. *Atmospheric Chemistry and Physics*, *13*(19), 10081–10094. https://doi.org/10.5194/acp-13-10081-2013

Frankignoul, C., Chouaib, N., & Liu, Z. (2011). Estimating the observed atmospheric response to SST anomalies: Maximum covariance analysis, generalized equilibrium feedback assessment, and maximum response estimation. *Journal of Climate*, *24*(10), 2523–2539. https://doi.org/10.1175/2010JCLI3696.1

Fuentes-Franco, R., Giorgi, F., Coppola, E., & Kucharski, F. (2016). The role of ENSO and PDO in variability of winter precipitation over North America from twenty first century CMIP5 projections. *Climate Dynamics*, *46*(9–10), 3259–3277. https://doi.org/10.1007/s00382-015-2767-y

Ge, J., Jia, X., & Ma, H. (2024). Pacific decadal oscillation modulation on the relationship between moderate El Niño-Southern Oscillation and East Asian winter temperature. *Atmosphere*, *15*(2), 228. https://doi.org/10.3390/atmos15020228

Gershunov, A., & Barnett, T. P. (1998). Interdecadal modulation of ENSO teleconnections. *Bulletin of the American Meteorological Society*, *79*(12), 2715–2725. https://doi.org/10.1175/1520-0477(1998)079<2715:imoet>2.0.co;2

Guan, X., Huang, J., Guo, R., & Lin, P. (2015). The role of dynamically induced variability in the recent warming trend slowdown over the Northern Hemisphere. *Scientific Reports*, *5*(1), 12669. https://doi.org/10.1038/srep12669

Guo, R., Huang, J., Yu, H., Zhao, H., & Hu, Z. (2024). Decadal modulation of temperature pattern over East Asia by Pacific decadal Oscillation. *Atmospheric Research*, *300*, 107248. https://doi.org/10.1016/j.atmosres.2024.107248

Harris, I., Osborn, T. J., Jones, P., & Lister, D. (2020). Version 4 of the CRU TS monthly high-resolution gridded multivariate climate dataset. *Scientific Data*, *7*(1), 109. https://doi.org/10.1038/s41597-020-0453-3

Hersbach, H., Bell, B., Berrisford, P., Hirahara, S., Horányi, A., Muñoz-Sabater, J., et al. (2020). The ERA5 global reanalysis [Dataset]. *Quarterly Journal of the Royal Meteorological Society*, *146*(730), 1999–2049. https://doi.org/10.1002/qj.3803

Hu, Y., Wang, S., Guan, X., & Huang, J. (2025). Distinct effects of soil moisture on surface water availability in nearshore and inland drylands. *Geophysical Research Letters*, *52*(20), e2025GL117631. https://doi.org/10.1029/2025gl117631

Huang, B., Thorne, P. W., Banzon, V. F., Boyer, T., Chepurin, G., Lawrimore, J. H., et al. (2017). *NOAA Extended Reconstructed Sea Surface Temperature (ERSST), Version 5. (indicate subset used)*. NOAA National Centers for Environmental Information. https://doi.org/10.7289/V5T72FNM

Huang, J., Guan, X., & Ji, F. (2012). Enhanced cold-season warming in semi-arid regions. *Atmospheric Chemistry and Physics*, *12*, 5391–5398. https://doi.org/10.5194/acp-12-5391-2012

Huang, J., Ji, M., Xie, Y., Wang, S., He, Y., & Ran, J. (2015). Global semi-arid climate change over last 60 years. *Climate Dynamics*, *46*(3–4), 1131–1150. https://doi.org/10.1007/s00382-015-2636-8

Huang, J., Li, Y., Fu, C., Chen, F., Fu, Q., Dai, A., et al. (2017). Dryland climate change: Recent progress and challenges. *Reviews of Geophysics*, *55*(3), 719–778. https://doi.org/10.1002/2016rg000550

Huang, J., Yu, H., Guan, X., Wang, G., & Guo, R. (2015). Accelerated dryland expansion under climate change. *Nature Climate Change*, *6*(2), 166–171. https://doi.org/10.1038/nclimate2837

IPCC. (2013). Climate change 2013: The physical science basis. In T. F. Stocker, D. Qin, G. K. Plattner, et al. (Eds.), *Contribution of working group I to the fifth assessment report of the intergovernmental panel on climate change*.

IPCC. (2023). Summary for policymakers. In H. Lee & J. Romero (Eds.), *Climate change 2023: Synthesis Report.Contribution of working groups I, II and III to the sixth assessment report of the intergovernmental Panel on climate change (core writing team* (pp. 1–34). IPCC. https://doi.org/10.59327/IPCC/AR6-9789291691647.001

Jamali, T., Ghanbarian, B., & Kurths, J. (2023). Spatiotemporal analysis of extreme precipitation events in the United States at mesoscale: Complex network theory. *Journal of Hydrology*, *627*, 130440. https://doi.org/10.1016/j.jhydrol.2023.130440

Jin, H., Zhang, K., Zhang, P., Liu, G., Liu, M., Chen, X., & Willems, P. (2025). Spatiotemporal evolution of drought status and its driving factors attribution in China. *Science of the Total Environment*, *958*, 178131. https://doi.org/10.1016/j.scitotenv.2024.178131

Kosaka, Y., & Xie, S.-P. (2013). Recent global-warming hiatus tied to equatorial Pacific surface cooling. *Nature*, *501*(7467), 403–407. https://doi.org/10.1038/nature12534

Lau, K. M., Lee, J. Y., Kim, K. M., & Kang, I. S. (2004). The North Pacific as a regulator of summertime climate over Eurasia and North America. *Journal of Climate*, *17*(4), 819–833. https://doi.org/10.1175/1520-0442(2004)017<0819:tnpaar>2.0.co;2

Lau, K. M., & Weng, H. (2002). Recurrent teleconnection patterns linking summertime precipitation variability over East Asia and North America. *Journal of the Meteorological Society of Japan*, *80*(6), 1309–1324. https://doi.org/10.2151/jmsj.80.1309

Lee, D. Y., Yeh, S. W., Jeong, H., & Park, H. S. (2025). Changes in the role of Pacific decadal oscillation on East Asian winter surface temperature. *Environmental Research Letters*, *20*(2), 024062. https://doi.org/10.1088/1748-9326/adaf45

Li, H., Dai, A., Zhou, T., & Lu, J. (2010). Responses of East Asian summer monsoon to historical SST and atmospheric forcing during 1950–2000. *Climate Dynamics*, *34*(4), 501–514. https://doi.org/10.1007/s00382-008-0482-7

Li, Y., Chen, Y., & Li, Z. (2019). Dry/wet pattern changes in global dryland areas over the past six decades. *Global and Planetary Change*, *178*, 184–192. https://doi.org/10.1016/j.gloplacha.2019.04.017

Mann, M. E., & Gleick, P. H. (2015). Climate change and California drought in the 21st century. *Proceedings of the National Academy of Sciences*, *112*(13), 3858–3859. https://doi.org/10.1073/pnas.1503667112

Mantua, N. J., Hare, S. R., Zhang, Y., Wallace, J. M., & Francis, R. C. (1997). A Pacific interdecadal climate oscillation with impacts on salmon production. *Bulletin of the American Meteorological Society*, *78*(6), 1069–1079. https://doi.org/10.1175/1520-0477(1997)078<1069:apicow>2.0.co;2

McCabe, G. J., Palecki, M. A., & Betancourt, J. L. (2004). Pacific and Atlantic Ocean influences on multidecadal drought frequency in the United States. *Proceedings of the National Academy of Sciences of the United States of America*, *101*(12), 4136–4141. https://doi.org/10.1073/pnas.0306738101

Newman, M., & Coauthors. (2016). The Pacific decadal oscillation, revisited. *Journal of Climate*, *29*, 4399–4427.

Qian, C., & Zhou, T. (2014). Multidecadal variability of North China aridity and its relationship to PDO during 1900–2010. *Journal of Climate*, *27*(3), 1210–1222. https://doi.org/10.1175/jcli-d-13-00235.1

Rotenberg, E., & Yakir, D. (2010). Contribution of semi-arid forests to the climate system. *Science*, *327*(5964), 451–454. https://doi.org/10.1126/science.1179998

Safriel, U., & Adeel, Z. (2005). Dryland systems. In R. Hassan, R. Scholes, & N. Ash (Eds.), *Ecosystems and human well-being*, *Current state and trends* (Vol. 1, pp. 625–658). Island Press.

Seager, R., Ting, M., Alexander, P., Liu, H., Nakamura, J., & Newman, M. (2023). Ocean-forcing of cool season precipitation drives ongoing and future decadal drought in southwestern North America. *npj Climate and Atmospheric Science*, *6*(1), 141. https://doi.org/10.1038/s41612-023-00461-9

Si, D., Jiang, D., & Ding, Y. (2021). Synergistic impacts of the Atlantic and Pacific Oceans on interdecadal variations of summer rainfall in Northeast Asia. *Journal of Meteorological Research*, *35*(5), 844–856. https://doi.org/10.1007/s13351-021-0191-2

Trenberth, K. E. (2015). Has there been a hiatus. *Science*, *349*(6249), 691–692. https://doi.org/10.1126/science.aac9225

Trenberth, K. E., Fasullo, J. T., & Shepherd, T. G. (2015). Attribution of climate extreme events. *Nature Climate Change*, *5*(8), 725–730. https://doi.org/10.1038/nclimate2657

Wang, N., Dee, S., Hu, J., Steiger, N., & Thirumalai, K. (2024). PDO and AMO modulation of the ENSO–Asian summer monsoon teleconnection during the last Millennium. *Journal of Geophysical Research: Atmospheres*, *129*(1), e2023JD039638. https://doi.org/10.1029/2023JD039638

Wang, S., Huang, J., Huang, G., Luo, F., Ren, Y., & He, Y. (2022). Enhanced impacts of Indian Ocean sea surface temperature on the dry/wet variations over Northwest China. *J. Geophy. Res.-Atmos.*, *127*(11), e2022JD036533. https://doi.org/10.1029/2022jd036533

Wang, S., Huang, J., He, Y., & Guan, Y. (2014). Combined effects of the Pacific decadal oscillation and El Nino-southern oscillation on global land dry–wet changes. *Scientific Reports*, *4*(1), 6651. https://doi.org/10.1038/srep06651

Yan, X., Cheng, P., Zhang, Q., Li, X., He, J., Yan, X., et al. (2022). Comparisons of climate change characteristics in typical arid regions of the Northern Hemisphere. *Frontiers of Environmental Science*, *10*, 1033326. https://doi.org/10.3389/fenvs.2022.1033326

Yang, S., Lau, K. M., & Kim, K. M. (2002). Variations of the East Asian jet stream and Asian-Pacific-American winter climate anomalies. *Journal of Climate*, *15*(3), 306–325. https://doi.org/10.1175/1520-0442(2002)015<0306:voteaj>2.0.co;2

Yu, B., & Zwiers, F. W. (2007). The impact of combined ENSO and PDO on the PNA climate: A 1,000-year climate modeling study. *Climate Dynamics*, *29*(7–8), 837–851. https://doi.org/10.1007/s00382-007-0267-4

Yu, L., Furevik, T., Otterå, O. H., & Gao, Y. (2015). Modulation of the Pacific Decadal Oscillation on the summer precipitation over East China: A comparison of observations to 600-years control run of Bergen Climate Model. *Climate Dynamics*, *44*(1–2), 475–494. https://doi.org/10.1007/s00382-014-2141-5

Zeng, N., Neelin, J. D., Lau, K. M., & Tucker, C. J. (1999). Enhancement of interdecadal climate variability in the Sahel by vegetation interaction. *Science*, *286*(5444), 1537–1540. https://doi.org/10.1126/science.286.5444.1537

Zhang, J., Wang, S., Huang, J., He, Y., & Ren, Y. (2023). The precipitation-recycling process enhanced extreme precipitation in Xinjiang, China. *Geophysical Research Letters*, *50*(15), e2023GL104324. https://doi.org/10.1029/2023GL104324

Zhang, L., & Zhou, T. (2015). Drought over east Asia: A review. *Journal of Climate*, *28*(8), 3375–3399. https://doi.org/10.1175/jcli-d-14-00259.1

Zhang, Q., Yang, J., Duan, X., Ma, P., Lu, G., Zhu, B., et al. (2022). The eastward expansion of the climate humidification trend in northwest China and the synergistic influences on the circulation mechanism. *Climate Dynamics*, *59*(7), 2481–2497. https://doi.org/10.1007/s00382-022-06221-4

Zhang, Y., Wallace, J. M., & Battisti, D. S. (1997). ENSO-like interdecadal variability: 1900–93. *Journal of Climate*, *10*(5), 1004–1020. https://doi.org/10.1175/1520-0442(1997)010<1004:eliv>2.0.co;2

Zhang, Y., Xie, S., Kosaka, Y., & Yang, J. (2018). Pacific decadal oscillation: Tropical Pacific forcing versus internal variability. *Journal of Climate*, *31*(20), 8265–8279. https://doi.org/10.1175/jcli-d-18-0164.1